

## ACCEPTED VERSION

Zhao Feng Tian, Graham J. Nathan, Yuchuan Cao

### **Numerical modelling of flows in a solar-enhanced vortex gasifier: Part 1, comparison of turbulence models**

Progress in Computational Fluid Dynamics, 2015; 15(2):114-122

Copyright © 2016 Inderscience Enterprises Ltd.

Published version at: <http://dx.doi.org/10.1504/PCFD.2015.068819>

#### **PERMISSIONS**

<https://www.inderscience.com/mobile/inauthors/index.php?pid=74>

*Accepted Manuscript\**

- Internally sharing the *Accepted Manuscript* within their research collaboration groups only, at any point after publication
- Posting the *Accepted Manuscript* on institutional repositories and/or subject repositories, subject to an embargo of *12 months* after publication (Green Open Access)
- Posting the *Accepted Manuscript* on academic social networks or social media, subject to an embargo of *24 months* after publication (Green Open Access)

**8 January 2024**

<http://hdl.handle.net/2440/99166>

# Numerical modelling of flows in a Solar-Enhanced Vortex Gasifier: Part 1, Comparison of Turbulence Models

Zhao Feng Tian\*, Graham J Nathan, Yuchuan Cao

Centre for Energy Technology, School of Mechanical Engineering, The University of Adelaide, South Australia  
5005, Australia

Email Address: zhao.tian@adelaide.edu.au

## ABSTRACT

The present paper reports the evaluation of performance of a series of turbulence models for an isothermal flow in a solar chemical reactor. This chemical reactor has similar swirling flow patterns to those in a solar-enhanced vortex gasifier (SVG) and measurements of velocity in this reactor are available in literature. Three turbulence models, namely, standard k- $\epsilon$  model, baseline (BSL) Reynolds stress model, and shear-stress-transport (SST) model are used to simulate the flows in the solar chemical reactor. It is found that the predictions of the three models are in reasonable agreement with the experimental data, although none are entirely satisfactory, with the predictions of the SST model being slightly better than those of the other models. However, even the SST model is not able to predict the anisotropic Reynolds stresses in the flow. More detailed measurements of flow fields in SVG type reactors are required for further evaluation.

## INTRODUCTION

Solar-driven gasification is an emerging technology to transform carbonaceous feedstocks, including those of low grade, into synthesis gas, also known as “syngas”. Several types of solar gasifiers have been proposed, developed and tested at the laboratory and pilot scales, notably the indirectly irradiated packed bed reactor, the directly irradiated vortex flow reactor and the indirectly irradiated entrained flow reactor (Piatkowski, Wieckert *et al.* 2011). Of these gasifiers, the directly irradiated vortex flow reactor, which is also called the solar enhanced vortex gasifier (SVG), is found to have the highest energy conversion efficiency (Piatkowski, Wieckert *et al.* 2011). However, despite its potential, further understanding of the flow-field within it is required to resolve the challenge of particle deposition on the window used to seal the reactor.

Steinfeld and co-workers at ETH, Zurich have developed a laboratory-scale SVG and evaluated it using both experimental measurements and modelling methods since the 90's. Figure 1 shows one of the computational fluid dynamics (CFD) model developed by the authors based on the SVG of Steinfeld' group (Z'Graggen and Steinfeld 2008). The SVG incorporates a quartz window mounted at the mouth of a front cone, a cylindrical reactor cavity and an aperture connecting them. Carbonaceous particles and water/steam are injected from one particle feeding inlet and steam injection ports, respectively. The flow of the steam and particles drives a vortex flow in the reactor as a result of their tangential components of inlet velocities. The concentrated solar radiation passes through the quartz window and the aperture to be absorbed by the particles within the reactor cavity.

The main functions of the quartz window are to control the atmosphere in the gasifier and prevent the egress of particles from it. However, the window is vulnerable both to the deposition of particles and to the condensation of steam onto it. Deposited particles reduce the transmissivity of the quartz window. Not only does this reduce efficiency, more importantly, it also leads to high local temperatures and greatly increases the risk that window will fail. Purging nozzles are therefore installed into the Front Cone, through which a purge gas is injected, with a view to cooling the window and preventing particle deposition (Z'Graggen 2008). However, the purging flows employed to date have been less than 100% effective, so that there is a need for further research to devise better solutions.

One potential alternative approach to avoiding the risk of particle deposition in the quartz window for the case of atmospheric pressure reactors, is to replace the quartz window with an aerodynamic device, such as a sealing gas curtain to keep the particles in the reactor. This also requires control of the complex aerodynamics in the reactor. The use of validated CFD models is an attractive way to perform this optimisation because, relative to the experimental methods, they offer faster, cheaper and more detailed information of fluid velocities, temperature distribution and particle concentrations. To the best knowledge of the authors, however, only a few CFD studies of the SVG have been reported in literature and these have been only partially validated. Z'Graggen et al. (Z'Graggen and Steinfeld 2008) developed a two-phase reactor model and used it to optimize the geometrical configuration and operational parameters such as the feedstock's initial particle size, feed rates and solar power input. The calculated temperature distribution, steam conversion rates and carbon conversion rates were validated against experimental data. Ozalp and Jayakrishna (Ozalp and JayaKrishna 2010) studied the influence of a helical vane on the flow field of a vortex solar reactor. Shilapuram et al. (Ozalp, Chien *et al.* 2013) simulated the residence time distribution and flow fields in an aerodynamically shielded solar cyclone reactor that is similar to the SVG but without the front cone or a quartz window. However, no validation of the flow-field, such as velocities and flow patterns, was reported in these papers, consistent with no detailed data of the flow field being available.

In the absence of detailed data of the flow field in the SVG, a CFD model of an alternative solar chemical reactor developed by Meier et al. (Meier, Ganz *et al.* 1996) was chosen for model development and validation. This solar chemical reactor, shown in Figure 2, has many similar features to the SVG and also generates a swirling flow-field. Furthermore, sufficient details of the geometry and measurements of the isothermal gas flows are reported to enable model development and validation. For these reasons, the aim of the present paper is to compare for the Meier reactor, the performance of the standard  $k-\epsilon$  model, the Renormalization group (RNG)  $k-\epsilon$  model, the SSG Reynolds stress turbulence model, the baseline Reynolds stress turbulence model (BSL RSM) and the Shear-Stress-Transport (SST) model. In particular we aim to compare the predictions against measurements for isothermal air flow velocity magnitude at four locations in the reactor.

## **MODEL DESCRIPTION**

Figure 2 presents the geometry of the Meier reactor, which was modelled using the software ANSYS/Designmodeler 14.0. The dimensions are based on available data from the literature (Meier, Ganz *et al.* 1996). The length of the cylindrical cavity of the reactor from the aperture plane to the outlet is 0.35 m. The diameters of the reactor cavity and the open (window-less) inlet are 0.25 m. The diameter of aperture (at the planes of the Radial inlet in Figure 2) is 0.1m. Air flows into the reactor through three nozzles (jet inlets in Figure 2), one open inlet, two tangential nozzles (tangential inlets shown in Figure 2) and one radial inlet. It is important to note that there is no quartz window in this reactor, so that ambient air can be induced to flow into or out-from the reactor through this open window inlet. The diameters of each jet inlet and that of the tangential inlet are 0.0015 m. The width of the radial inlet is 0.0002 m. Air flows out of the reactor through a pipe (outlet in Figure 2). The diameter of the outlet pipe is 0.01 m.

Table 1 lists the detailed conditions for the boundaries. More details of dimensions and boundary conditions can be found in (Meier, Ganz *et al.* 1996). The ANSYS/Meshing tool was used to generate the unstructured mesh shown in Figure 4. The mesh quality was checked for skewness, aspect ratio, orthogonality and expansion factor. The influence of mesh node numbers on the CFD results were tested in a series of meshes, as is reported below. The commercial CFD software ANSYS/CFX 14 (Ansys 2011) was employed to predict the steady state air flows in the reactor. The governing equations were discretised using the finite-volume approach. The discretisation, High resolution scheme, was employed in the simulations. The convergence criteria for the air phase properties were set to  $1 \times 10^{-5}$  of the RMS. The convergence was further checked by verifying that the global quantities such as the pressure difference between the open window inlet and outlet was nearly constant.

## **Results and discussions**

### **Mesh refinement test**

A preliminary mesh of the reactor geometry was generated with a mesh of 0.5 million mesh nodes. A series of mesh refinements were conducted on the same geometry using 0.8 million, 1.17 million, 1.7 million and 2.15 million mesh nodes. When generating the meshes, the so-called ‘inflation’ layers were used for all wall boundaries in order to better resolve the boundary layers.

To test the effects of the mesh node number on the CFD result, the airflows in the reactor were simulated based on the different meshes using the SST model. Figure 4 shows the predicted velocity contour at the mid plane of the reactor based on the 2.15 million node mesh. In the experiment of (Meier, Ganz *et al.* 1996), velocity vector magnitudes were measured along four lines at the axial locations of  $x = 0.03$  m, 0.07 m, 0.11 m and 0.16 m as shown in Figure 4. Figures 5a and 5b compare

the velocity magnitudes along line  $x = 0.03$  m and  $x = 0.16$  m, respectively, based on the finest three meshes. At  $x = 0.03$  m, there is slight discrepancy between the 2.15 million mesh and 1.7 million mesh results. However, it can be seen that the simulated results at  $x = 0.16$  m based on the 1.7 million mesh are very close to the results based on the 2.15 million mesh. The mesh of 2.15 million nodes was therefore chosen to compare the performance of the different turbulence models.

### Comparison of different turbulence models

It was found that, for the 2.15 million node mesh, sufficient converge of the model was not achieved with the RNG  $k-\varepsilon$  or with the SSG Reynolds stress turbulence models, even for a range of different Timescale factors. Therefore only the results based on standard  $k-\varepsilon$  model, SST model and BSL RSM model are reported here.

Figure 6 compares the simulated velocity magnitudes with the measured data along the four radial traverses (see Figure 4). At  $x = 0.03$  m, the Standard  $k-\varepsilon$  model is found to over-predict the velocity at  $r/R = 0.05$  by about 54% , at  $r/R = 0.14$  by about 68% and at  $r/R = 0.22$  by about 44%, while it under-predicts the velocity at  $r/R = 0.3$  by about 24% and  $r/R = 0.42$  by about 27%. Similarly, the SST model also over-predicts the velocity magnitude at  $r/R = 0.05$  by about 27% , at  $r/R = 0.14$  by about 37% and at  $r/R = 0.22$  by about 19%, while it under-predicts the velocity magnitude at  $r/R = 0.3$  by about 27% and  $r/R = 0.42$  by about 21%. The BSL Reynolds stress model over-predicts the mean velocity at all measured locations. However, the trend of the flow pattern predicted by the BSL RSM is most similar to that of the experiment. Importantly, no data are available in the region  $r/R > 0.7$ , where the models predict a significantly higher velocity, so that it is not possible to fully assess the models at this axial plane.

Figure 6b presents the same comparison at  $x = 0.07$  m. It can be seen that all three models over-predict the velocity magnitude at  $r/R = 0.1$ . The results based on SST model are in very good agreement with the measurements at other measuring locations for which data are available, while predictions based on BSL Reynolds stress model and standard  $k-\varepsilon$  model are slightly different from the experimental data. However, for this profile, data are not available for  $r/R > 0.7$ , where all three models predict significant gradients in the radial profile.

At  $x = 0.11$  m (Fig 6c), all three models significantly over-predict the velocity magnitude at  $r/R = 0.84$  and  $r/R = 0.97$ . At  $r/R = 0.84$ , the SST model over-predicts the velocity by about 207%, the BSL model by 206% and the standard  $k-\varepsilon$  model by 111%. At  $r/R = 0.97$ , the SST model over-predicts the velocity by as high as 220%, the BSL model by 206% and the standard  $k-\varepsilon$  model by 147%. All three models under-predict the velocity magnitude at  $r/R = 0.515$  by 28% (SST model), 33% (Standard  $k-\varepsilon$  model) and 45% (BSL model). All models are unable to reproduce the velocity trend along this line, predicting a peak velocity close to the wall, where the experiment reports a relatively low velocity. At  $x = 0.16$  m (Fig 6d), all three models over-predict the velocity magnitude at all measured locations. However, all models successfully reproduce the

velocity trend along this line. A closer observation reveals that results from the Standard  $k$ - $\epsilon$  model agree best with the measurements. Also at this location, experimental data are not available at  $r/R < 0.4$ , where once again the models predict relatively large gradients in velocity.

Generally, all three models give predictions that are in reasonable agreement with the measurements except at the line  $x = 0.11$  m. The flow trends along the other lines in the reactor are captured by the models. Of the three models, the SST model provides the best agreement with the measurements at  $x = 0.03$  m and  $x = 0.07$  m.

### Further discussions

The flow in this vortex flow furnace is very complex, including strong swirling flows, impinging flows and jets. For example, Figure 4 shows that an air jet enters the chamber at a velocity of 120 m/s and impinges on the cone to form a 'wall jet', before separating from the cone to form a free jet. Previous work has shown that two equations RANS models with eddy viscosity are unable to predict reliably the anisotropic Reynolds stresses that can be found in impinging flows, due to the isotropic eddy viscosity assumption (Craft, Graham *et al.* 1993). As shown in Equation 1, based on the Boussinesq hypothesis, Reynolds Stresses are assumed to be proportional to the strain rate in the eddy viscosity models

$$\tau_{ij} = \mu_t \left[ \left( \frac{\partial u_i}{\partial x_j} + \frac{\partial u_j}{\partial x_i} \right) - \frac{2}{3} \delta_{ij} \rho k \right] \quad (1)$$

where  $\tau_{ij}$  is Reynolds stress,  $u_i$  is velocity in  $x_i$  coordinate,  $\rho$  is the density of fluid,  $k$  is turbulence kinetic energy,  $\mu_t$  is turbulence viscosity that is calculated from  $k$  and  $\epsilon$  for  $k$ - $\epsilon$  model, e.g.  $\mu_t = \rho C_\mu \frac{k^2}{\epsilon}$  or from  $k$  and  $\omega$  for SST model,  $\delta_{ij}$  is

Kronecker delta that equals 1 when  $i = j$  and 0 when  $i \neq j$ .

The second term of the right hand side of Equation 2,  $-\frac{2}{3} \delta_{ij} \rho k$ , ensures that the sum of all normal stresses is  $-\rho k$  (Versteeg 1995). However, this assumes the normal Reynolds stresses to be isotropic, which is inaccurate in the conditions that apply in this flow. In contrast, the BSL RSM model calculates each Reynolds stress term by solving extra transport equations, together with the turbulence frequency  $\omega$ . Therefore, the BSL RSM model accounts for the anisotropic Reynolds stresses that may be present in the flow. Figure 7 shows the predicted Reynolds stresses based on BSL RSM model along the line  $x = 0.16$  m. The normal Reynolds stress  $\tau_{xx}$  ( $uu$  in the Figure) is calculated to be as much as twice of the normal Reynolds stress  $\tau_{yy}$  ( $vv$

in the Figure) and also much higher than  $\tau_{ww}$  ( $ww$  in the Figure). This provides good reason to question the validity of the  $k-\varepsilon$  and the SST models, both of which assume the normal Reynolds stresses to be identical.

Figure 8 shows the predicted swirl number along axial direction ( $x$  coordinate in Figure 4) in the reactor by both SST model and BSL RSM model. The swirl number is defined as

$$S = \frac{\int U_x U_\theta r dA}{R \int U_x^2 dA} \quad (2)$$

where,  $U_x$  is the axial velocity,  $U_\theta$  is tangential velocity at corresponding radial position  $r$  and  $R$  is the diameter of the reactor cavity.

The calculations also find very strong gradients in the local swirl number, so that the flow undergoes a transition from strongly swirling to weakly swirling flow in a short distance. At  $x = 0.24$  m, where the tangential inlets are located (see Figure 2), the air flows from the tangential inlets form a strong swirling flow. The SST model predicts a swirl number of 4.29, which is close to that predicted by the BSL RSM of 4.75. The swirl number is predicted by both models to decrease strongly with axial distance to  $S=1.02$  for BSL RSM and  $S=0.77$  for the SST model at  $x = 0.179$  m. The swirl number is then calculated to plunge further to  $S \approx 0.16$  (BSL RSM) and  $0.13$  (SST model) at  $x = 0.174$  m, in which is the inlet plane for the jets. The significant drop of swirl number here is due to the introduction of axial fluid through the jet inlets. The swirl number is then calculated to decrease gradually to about  $0.068$  (BSL RSM) and  $0.038$  (SST model) at  $x = 0.03$  m. This strong gradient in swirl number also makes the flow very complex.

To take into consideration of the effects of streamline curvature in swirling flows, Smirnov and Menter (Smirnov and Menter 2009) developed a curvature correction for the SST model. Figure 9 compares the predicted velocity magnitude at  $x= 0.03$  m and  $x = 0.07$  m for the cases with and without this correction term. It can be seen that the SST model with curvature correction provides results that are in better agreement with the measurements than for the SST model without the curvature correction.

Further assessment of the relative performance of the models in another relevant configuration have also recently become available in another swirling flow solar reactor (Ozalp, Chien *et al.* 2013). Detailed flow field measurements including tangential and axial velocities and vorticity field are reported in the experiment, making more detailed analysis of CFD models possible.

## CONCLUSION

The complexity of the flow-field in a vortex flow reactor makes reliable predictions a challenge for all RANS models tested in the paper. In particular, the simulations performed with the RNG  $k-\varepsilon$  and the SSG RSM models failed to converge sufficiently. The three turbulence models that did yield reasonable convergence are the standard  $k-\varepsilon$  model, the SST model and the BSL RSM model. These three models were found to yield reasonable agreement with the limited available experimental data, although none are entirely satisfactory. A close inspection shows that the SST model with curvature correction provides slightly better agreement of the mean flow-field than do the other models. However, the SST model can not predict the anisotropic Reynolds stresses, due to its reliance on the eddy viscosity concept. The BSL RSM that solves the transport equations of each Reynolds stresses overcomes this shortcoming, but this does not make it more accurate in predicting the mean flow-field.

A more detailed analysis of the performance of the various models in predicting parameters such as second moments and swirl numbers, is not possible since only the mean velocity is reported – and then only along four traverses. Further assessments will be reported using more detailed measurements of the fluid fields that have recently become available.

## ACKNOWLEDGEMENT

The authors will acknowledge the financial support from the Australian Research Council.

## REFERENCES

- Ansys AC (2011) 14.0 Theory Guide. ANSYS inc.
- Craft T, Graham L, Launder BE (1993) Impinging jet studies for turbulence model assessment—II. An examination of the performance of four turbulence models. *International Journal of Heat and Mass Transfer* **36**(10), 2685-2697.
- Meier A, Ganz J, Steinfeld A (1996) Modeling of a novel high-temperature solar chemical reactor. *Chemical engineering science* **51**(11), 3181-3186.
- Ozalp N, Chien M-H, Morrison G (2013) Computational Fluid Dynamics and Particle Image Velocimetry Characterization of a Solar Cyclone Reactor. *Journal of Solar Energy Engineering* **135**, 031003.
- Ozalp N, JayaKrishna D (2010) CFD analysis on the influence of helical carving in a vortex flow solar reactor. *International Journal of Hydrogen Energy* **35**(12), 6248-6260.
- Piatkowski N, Wieckert C, Weimer AW, Steinfeld A (2011) Solar-driven gasification of carbonaceous feedstock-a review. *Energy & Environmental Science* **4**(1), 73-82.
- Smirnov PE, Menter FR (2009) Sensitization of the SST turbulence model to rotation and curvature by applying the Spalart-Shur correction term. *Journal of turbomachinery* **131**(4).
- Versteeg HK (1995) 'An introduction to computational fluid dynamics the finite volume method, 2/E.' (Pearson Education India)
- Z'Graggen A (2008) Solar Gasification of Carbonaceous Materials: Reactor Design, Modeling and Experimentation. ETH,

Z'Graggen A, Steinfeld A (2008) Hydrogen production by steam-gasification of carbonaceous materials using concentrated solar energy–V. Reactor modeling, optimization, and scale-up. *International Journal of Hydrogen Energy* **33**(20), 5484-5492.

## **Biographies**

Dr. Zhao Feng Tian is a Lecturer in the School of Mechanical Engineering at the University of Adelaide. He received a Bachelor's Degree from Shanghai Jiaotong University, China, in 1997 and a Master's Degree from the University of New South Wales, Australia, in 2002. He attained his PhD in Mechanical Engineering at RMIT University, Australia in 2007. His research and teaching interests focus on computational fluid dynamics (CFD) and CFD modelling of engineering combustion.

Professor 'Gus' Nathan is professor of Mechanical Engineering and the founding director of the Centre for Energy Technology at the University of Adelaide. He received his BE(Hons) and his PhD from the University of Adelaide in 1985 and 1989, respectively. His research interest is in thermal fluid science and technology, specialising in the development and use of laser diagnostic methods in turbulent reacting flows and in the development of novel hybrid technologies between concentrated solar radiation and combustion or gasification.

Mr Yuchuan Cao is currently studying the Professional Year Program in Adelaide. He received Bachelor's Honour Degree in Aerospace and Mechanical Engineering and Master's Degree in Mechanical Engineering from the University of Adelaide in 2011 and 2012, respectively. His research interest is in computational fluid dynamics (CFD).

**Table 1:** Boundary Details.

Boundary type	Boundary Details
Windows Inlet	Mass flow rate 0.004583 kg/s
Radial Inlet	Normal velocity 5.7 m/s
Particle Inlets	Normal velocity 122 m/s
Tangential Inlets	Normal velocity 120 m/s



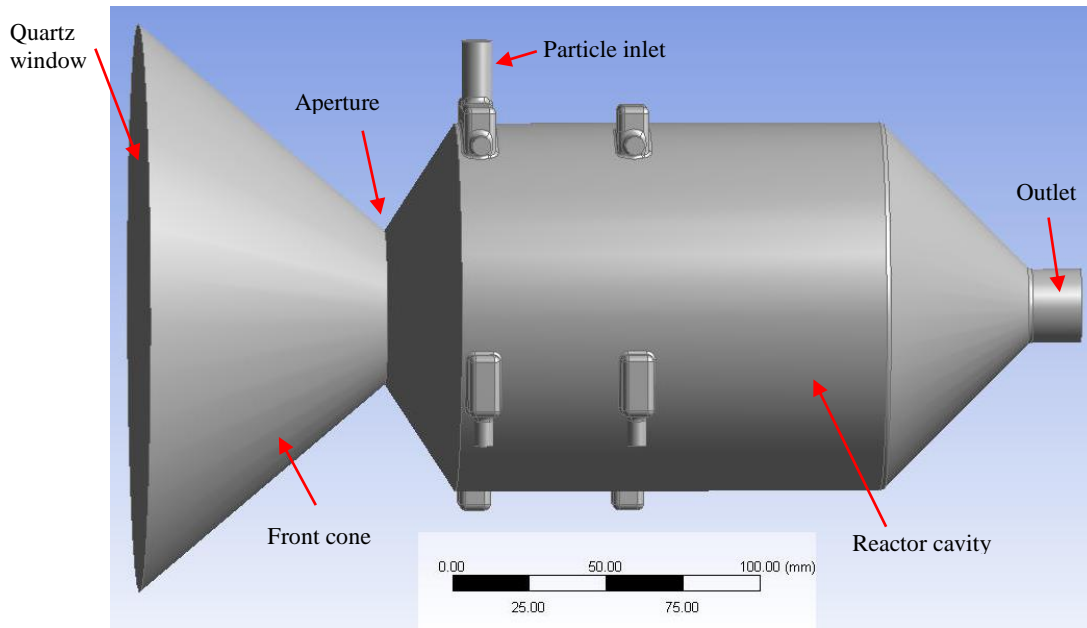


**Figure 1:** Geometry of the Solar-enhanced Vortex Gasifier (SVG) model (Z'Graggen and Steinfeld 2008).

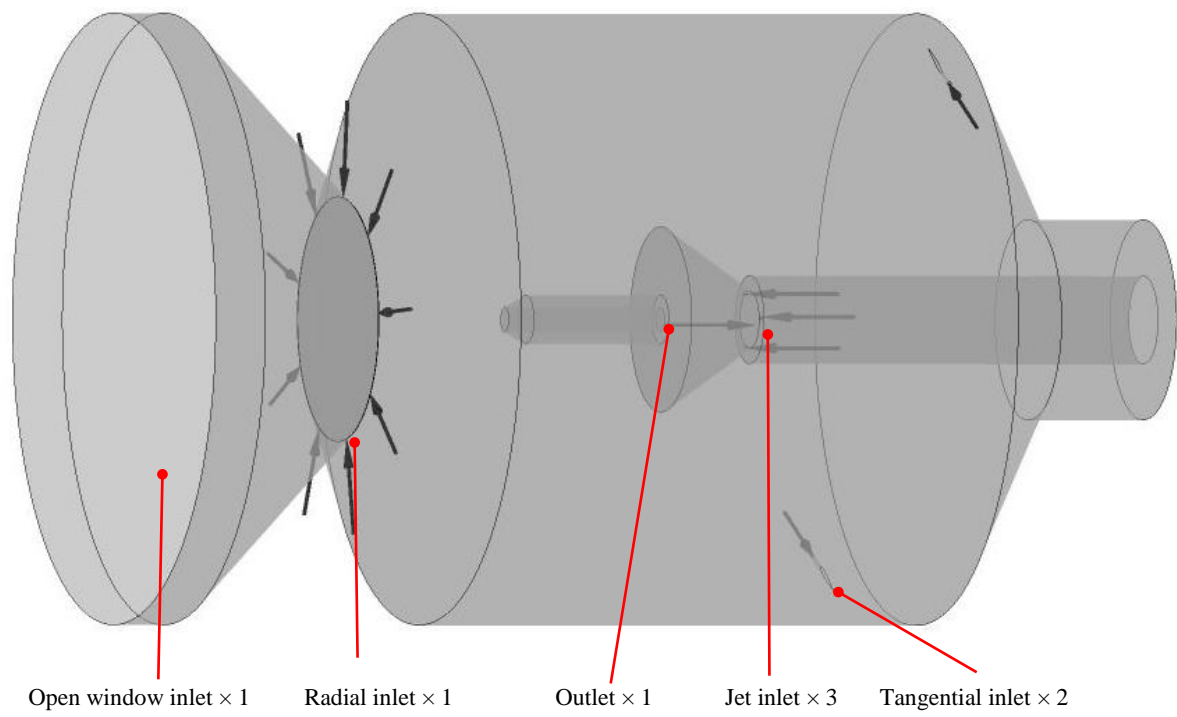


**Figure 2:** Schematic diagram of the reactor of (Meier, Ganz *et al.* 1996) chosen for model validation.

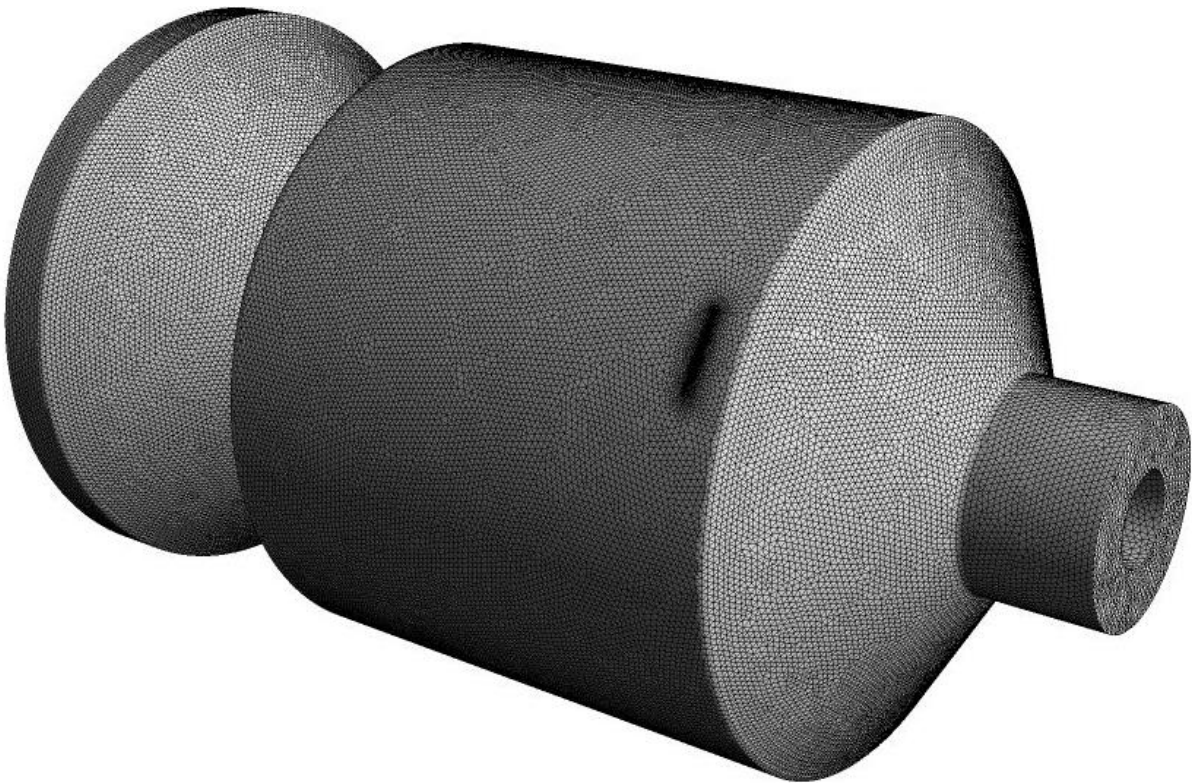
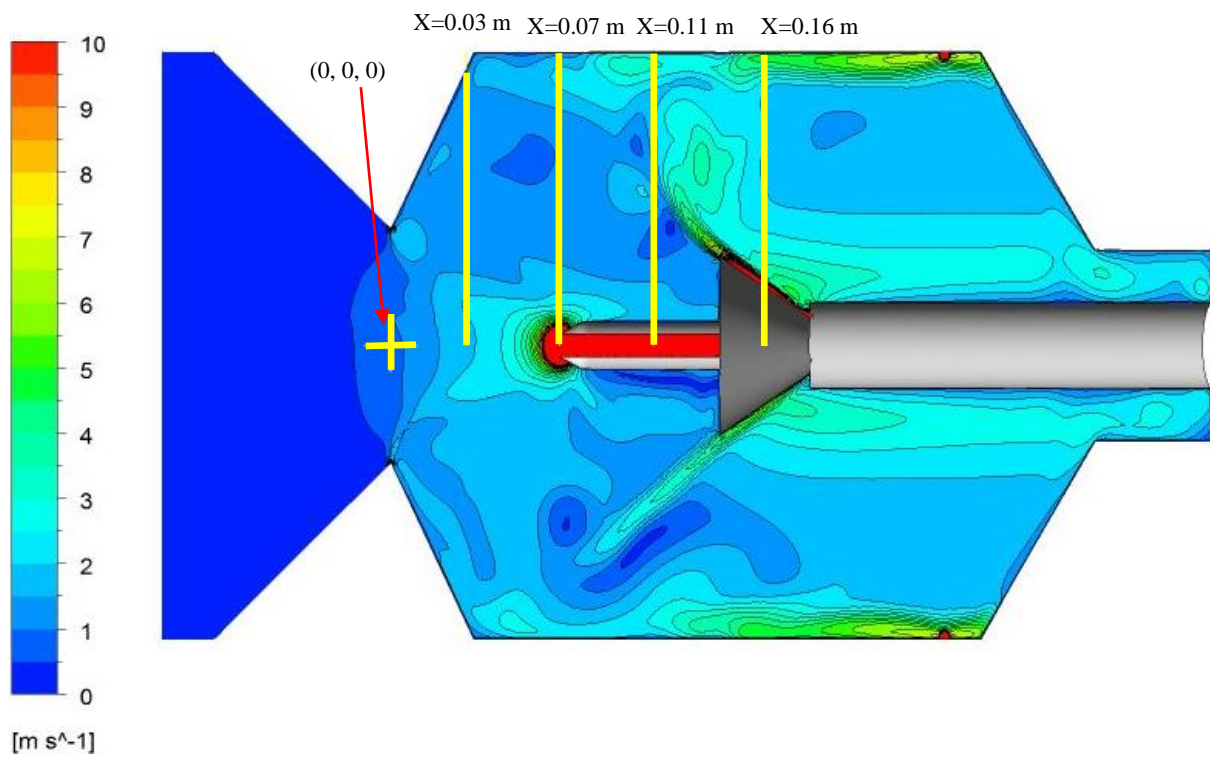
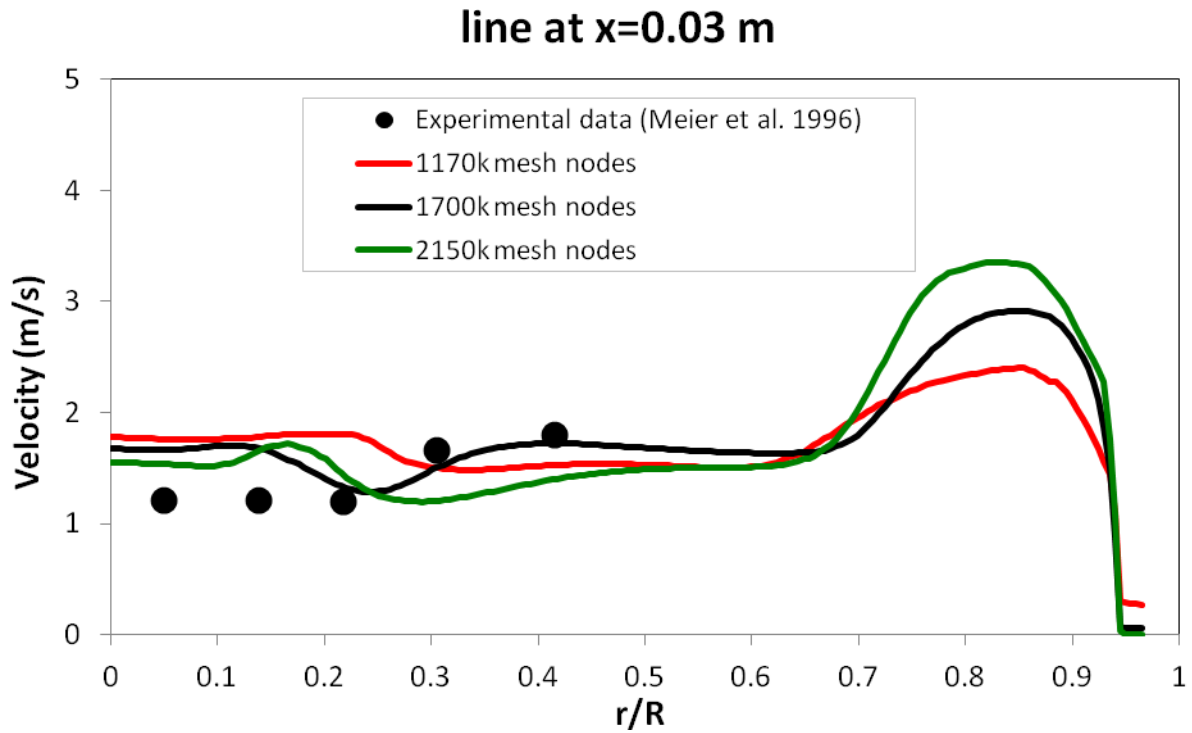


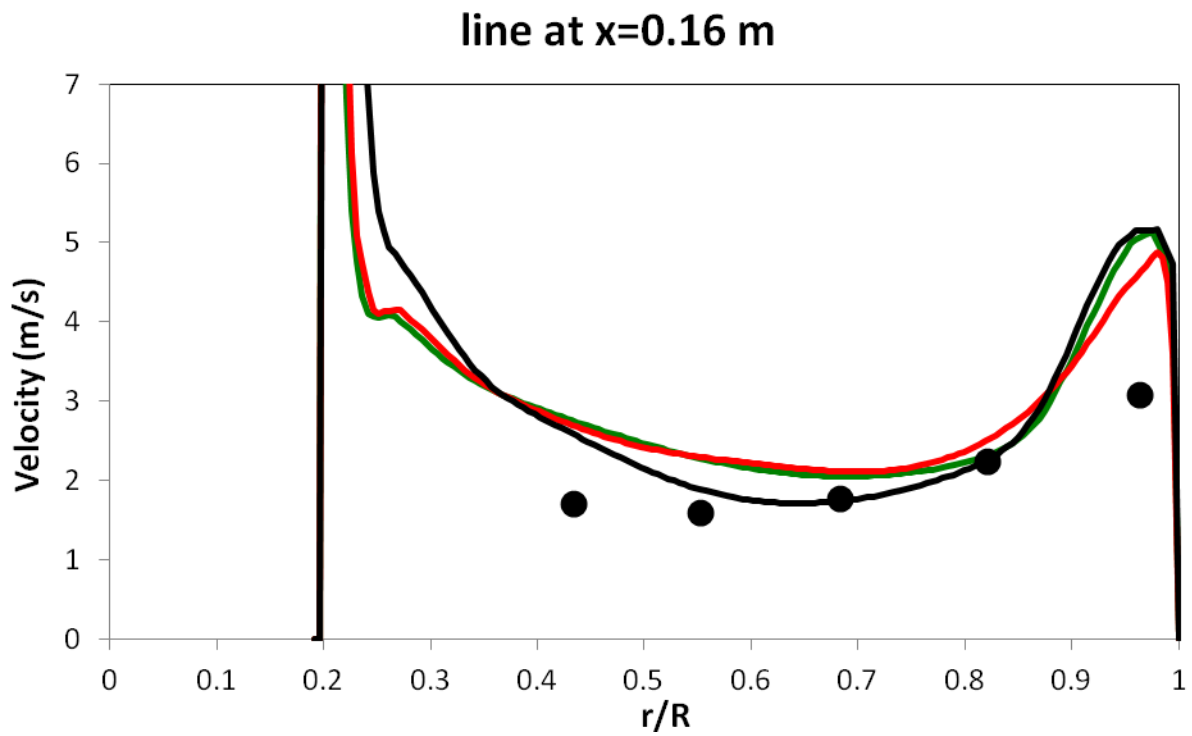
Figure 3: Mesh of the model (2.15 million mesh nodes).



**Figure 4:** The locations of the four traverses and the predicted velocity contour in the reactor, where  $x$  defines as the distance from the origin  $(0, 0, 0)$  to each traverse.



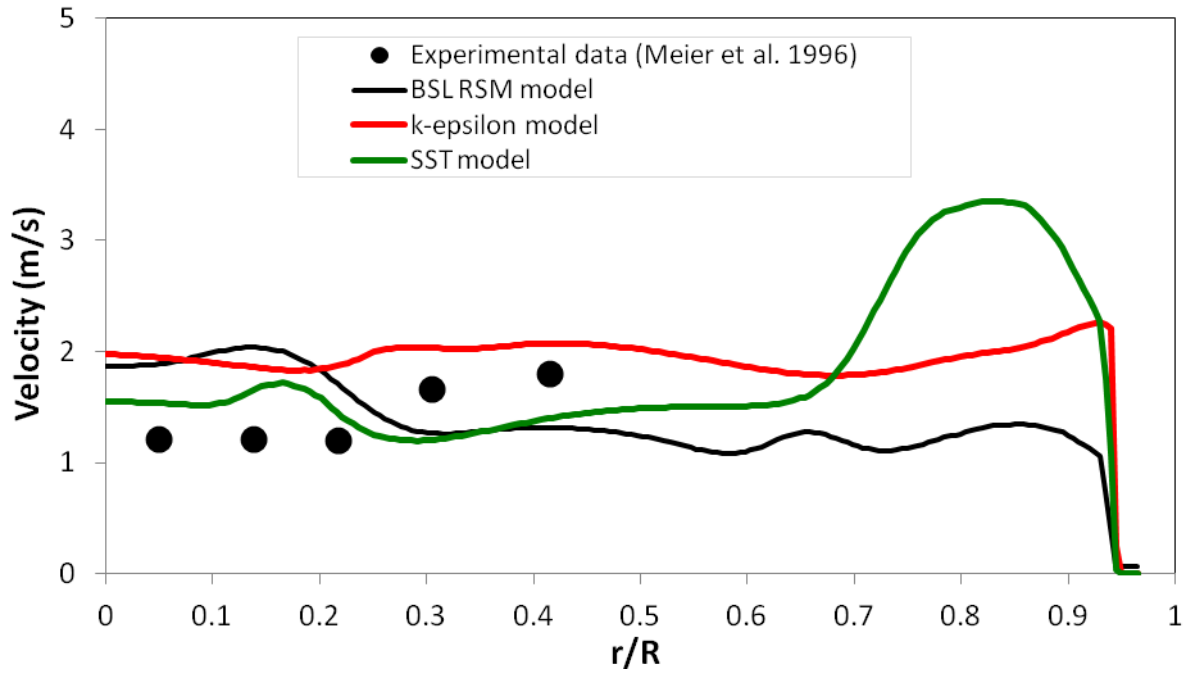
(a)



(b)

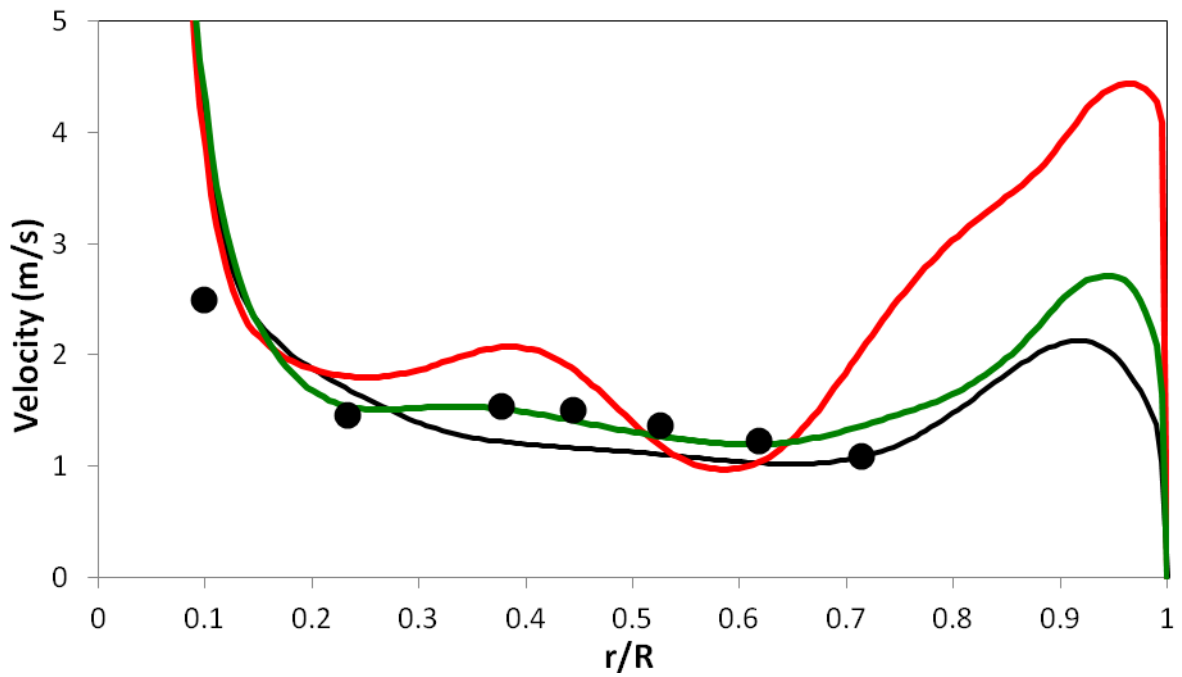
**Figure 5:** Comparison of CFD predictions for three levels of mesh refinement with experimental data along four radial traverses, where  $r$  is the radial distance from initial point and  $R$  is the radius of the reactor, 125mm.

### line at x=0.03 m



(a)

### line at x=0.07 m



(b)

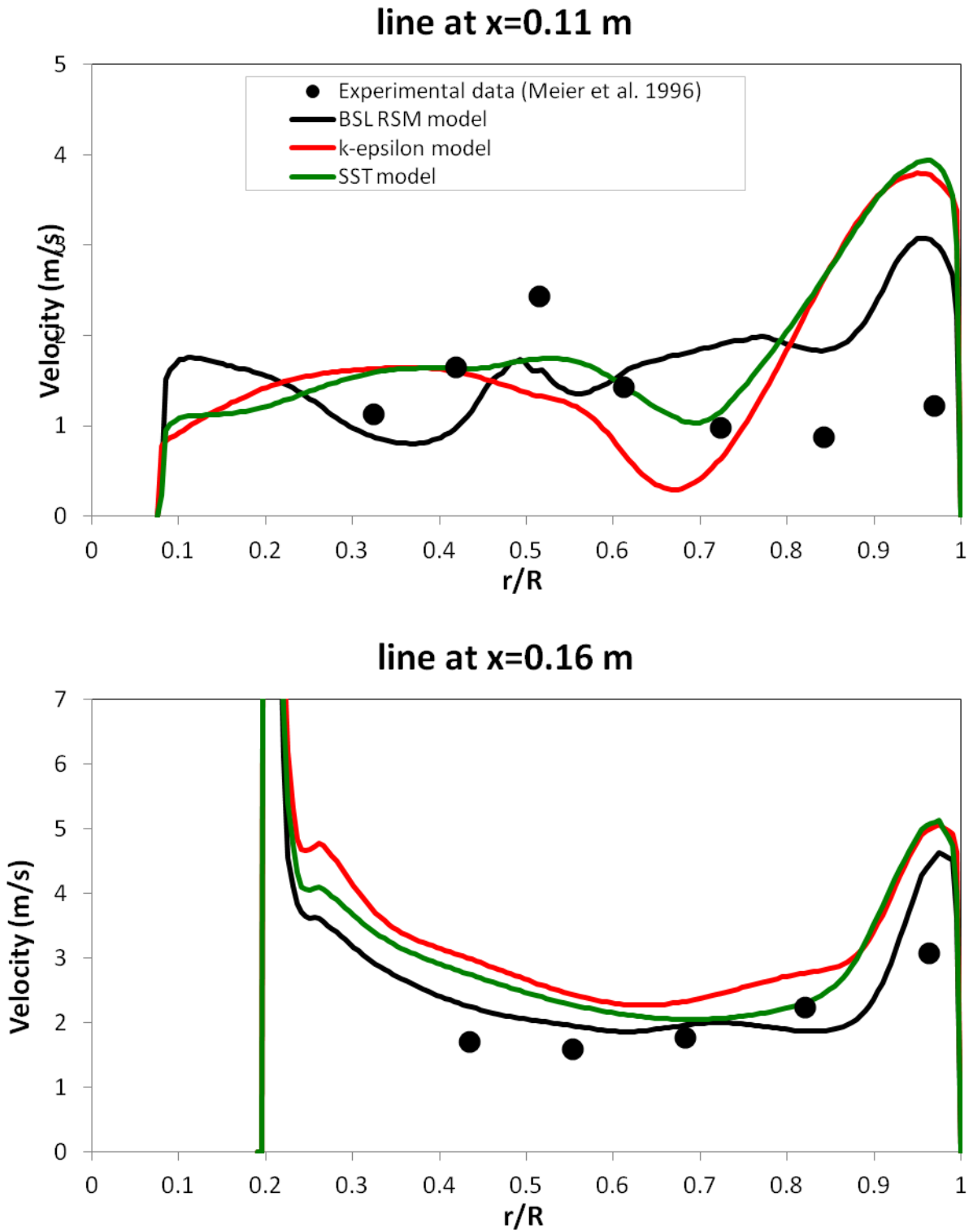


**Figure 6:** Comparison of CFD predictions with experimental data along four radial traverses, where  $r$  is the radial distance from initial point and  $R$  is the radius of the reactor, 125mm.

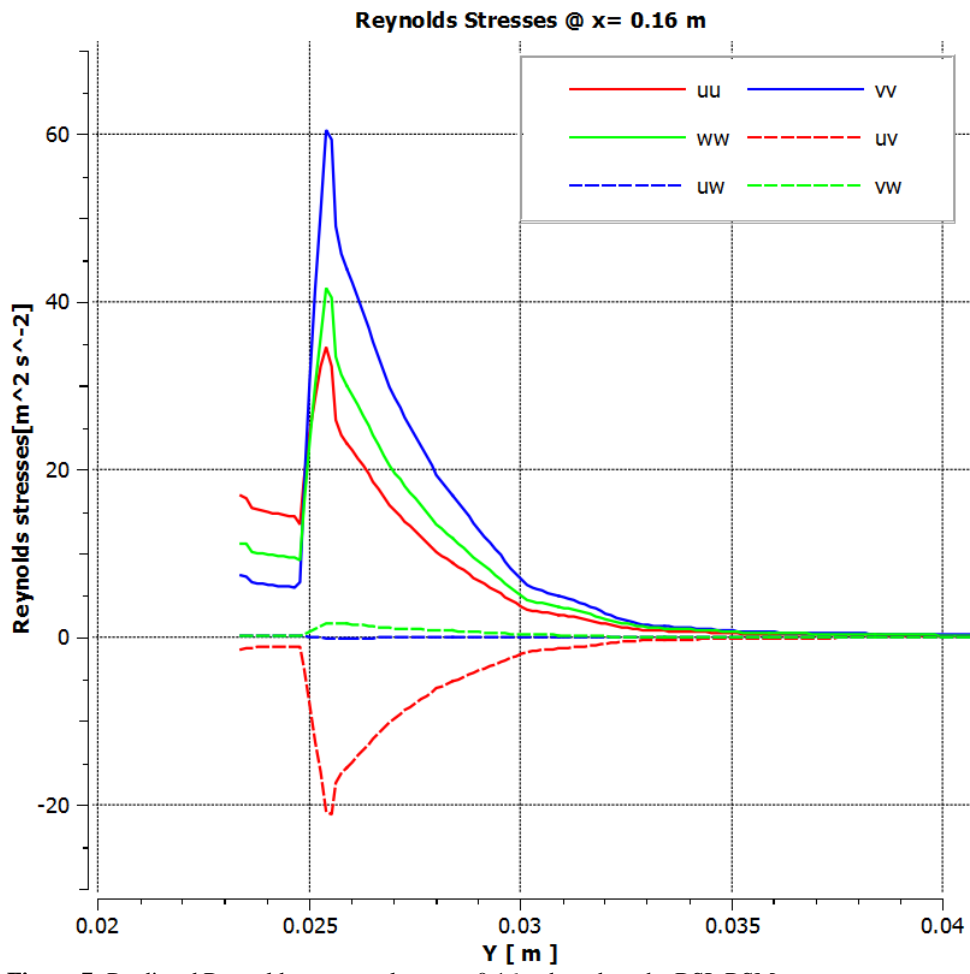
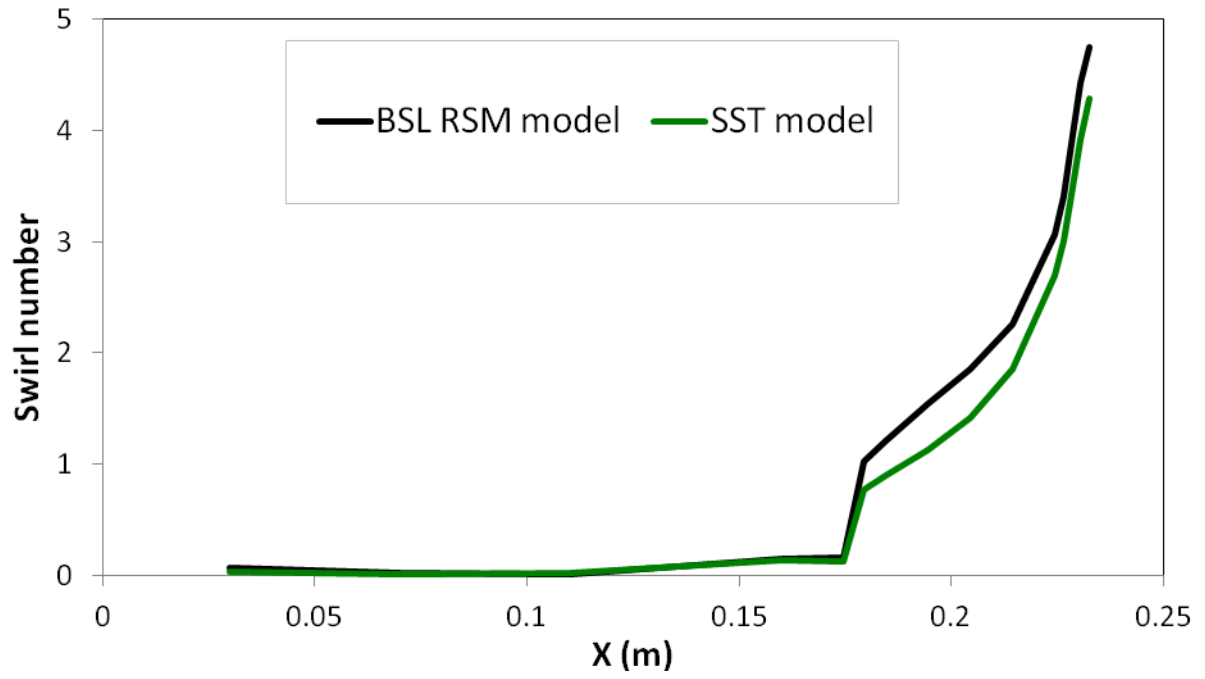
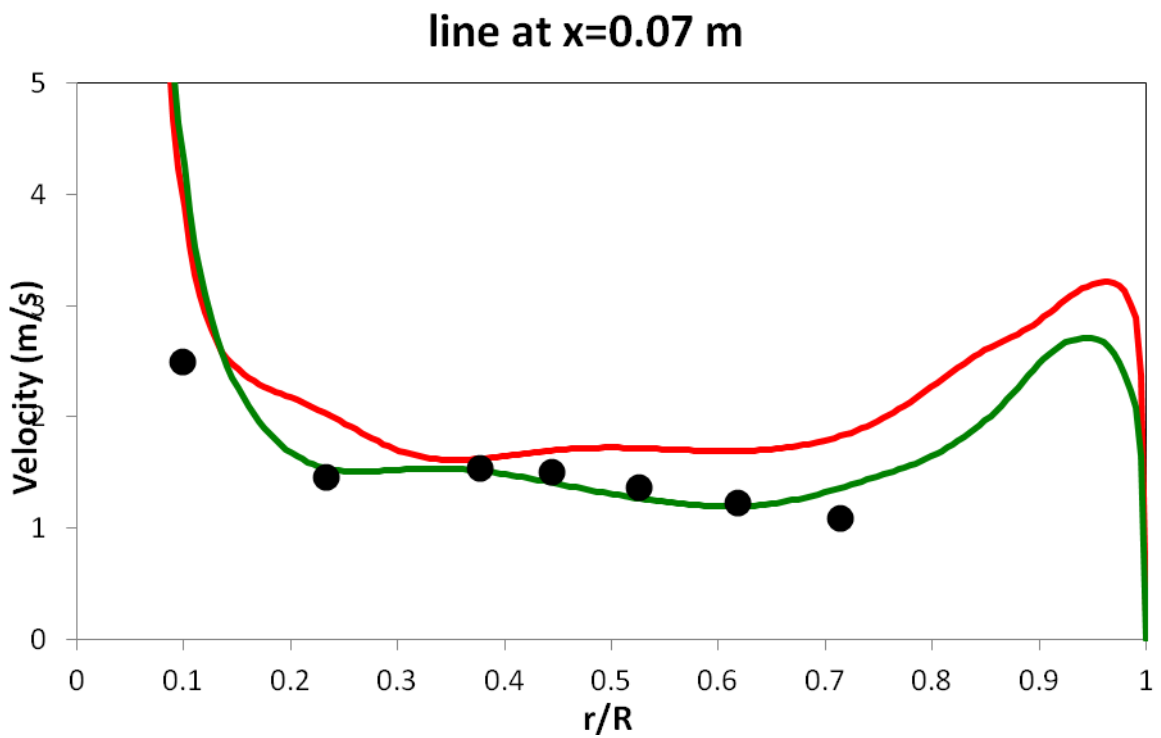
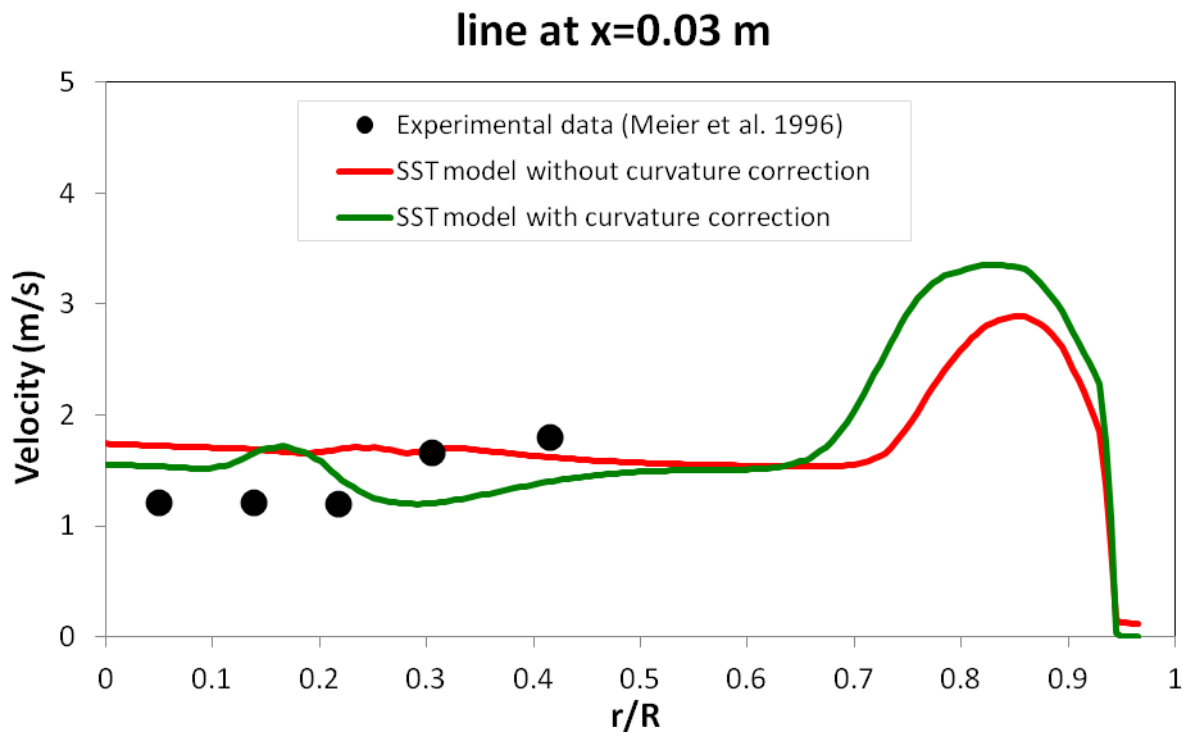


Figure 7: Predicted Reynolds stresses along x = 0.16 m based on the BSL RSM.



**Figure 8:** Predicted swirl number along axial direction in the furnace.



**Figure 9:** Effects of curvature correction on the SST model results.